frontiers

Supplementary Material: Petrological Geodynamics of Mantle Melting I. AlphaMELTS + Multiphase Flow: Dynamic Equilibrium Melting, Method and Results

Massimiliano Tirone, Jan Sessing

*Correspondence:
Max Tirone:
max.tirone@gmail.com

1 SUPPLEMENTARY DATA

The supplementary data provides a brief description and access to the data files of most of the numerical simulation that were performed for this study. Four animations illustrating the variation of some numerical results over time are also included.

The data repository link to access all the files is:
`https://figshare.com/collections/max-front1/3744383/1`

The movie file `mf1-movie1.PHASE33B.YRC5.avi` shows the results of the two-phase flow model discussed in section "Test of the Dynamic Model" which is based on a fixed input of melt at the bottom and does not include the thermodynamic computation. Number of spatial grid points is 500, time step is 250 yr, movie frames are recorded every 10 simulation time steps.

The movie file `mf1-movie2.PHASE3-P.BRC4-5.avi` illustrates some results of the dynamic batch melting model discussed in section "Results from the Dynamic Equilibrium Melting Model". The data file `PHASE3-P.BRC4-5.DAT` that can be found in the zip file `max-front1-data.zip` contains all the necessary information to create the animation. The data file includes also additional info. This particular simulation was computed with 300 spatial grid points, the thermodynamic computation was applied every 8 time steps.

All the data files that are made available with this study, are divided in blocks of data separated by a text starting with "ZONE". Each data block includes all the output info related to a particular time step. Each line of the block reports the information related to a particular depth point. A complete description of the data files can be found in `data-description.txt` included in the zip file `max-front1-data.zip` and `max-front1-data2.zip`.

Some of the results of two dynamic equilibrium melting (DEM) models coupled with the thermodynamic calculation presented in section "Results from the Dynamic Equilibrium Melting Model" are shown in the movie files `mf1-movie3.PHASE3-P.YRC4.avi` and `mf1-movie4.PHASE3-P2.YRC13.avi`. The main difference between the two animations is the viscosity of the solid matrix. In the first case $\mu^s = \mu_0^s$ with $\mu_0^s = 1e21$ Pa s. The second simulation assumes $\mu^s = \mu_0^s(1 + 1/\phi^m)$ with $\mu_0^s = 1e20$ Pa s. The number of grid points is 200, bottom velocity

of the solid is set to -0.03 m/yr (negative upwards) and bottom temperature 1450^{o}C. The permeability constant is 1e9 m^{-2}. The thermodynamic computation is applied every 8 time steps. The movies show the simulation results every 10 time steps. The data files used for the two movies are `PHASE3-P.YRC4.DAT`, included in the zip file `max-front1-data.zip`, and `PHASE3-P2.YRC13.DAT`, included in the zip file `max-front1-data2.zip`.

In the main text a list of all the relevant simulations that have been performed for this study can be found in Table 1. Most of the data files from these simulations are included in the zip files `max-front1-data.zip` and `max-front1-data2.zip`.

List of all the files in the supplementary material:

- `mf1-movie1.PHASE33B.YRC5.avi`
- `mf1-movie2.PHASE3-P.BRC4-5.avi`
- `mf1-movie3.PHASE3-P.YRC4.avi`
- `mf1-movie4.PHASE3-P2.YRC13.avi`
- `max-front1-data.zip`
- `max-front1-data2.zip`

2 DYNAMIC EQUILIBRIUM MELTING: EFFECT OF THE NUMBER OF GRID POINTS AND INTERVAL BETWEEN THERMODYNAMIC COMPUTATIONS

In the main text the effect of the number of grid points and the effect of the interval between thermodynamic computations have been investigated only for the dynamic melting model (Figure 2) and for the dynamic batch melting model (Figure 3). Here these effects are considered, to some extent, for the results of the DEM model. Since the number of available simulations that can be used for a comparison is rather limited (see Table 1 in the main text), only a preliminary assessment can be made.

Figure S1 shows the results using the model with $\mu^s = \mu_0^s$. The simulation with 200 grid points and nthermo = 8 (same as in Figure 7, main text) is compared with a simulation using 300 grid points and nthermo = 16 and another simulation with 200 grid points and nthermo = 4.

Two simulations using the model with $\mu^s = \mu_0^s(1 + 1/\phi^m)$ are shown in Figure S2 and Figure S3. The viscosity of the solid without melt is $\mu_0^s = 3e19$ Pa s. The first simulation has been carried out with 200 grid points and nthermo = 8 while the second simulation is based on 500 grid points and nthermo = 8. Data for all the simulations with the only exception of the one with 500 grid points are available following the instructions given in section 1.

3 VARIATION OF SELECTED SOLID MANTLE PROPERTIES AT THE TOP SIDE OF THE MODEL

Only a limited number of observations regarding the results of the DEM model have been presented in the main text. The data files of all the simulations provide the material for further independent analysis. For example Figure S4 shows a series of panels illustrating the variation of certain properties of the solid mantle at the exit point (top side) of the melt column. The corresponding variations in the melt can be found in Figure 7 (main text).

4 SUPPLEMENTARY FIGURES

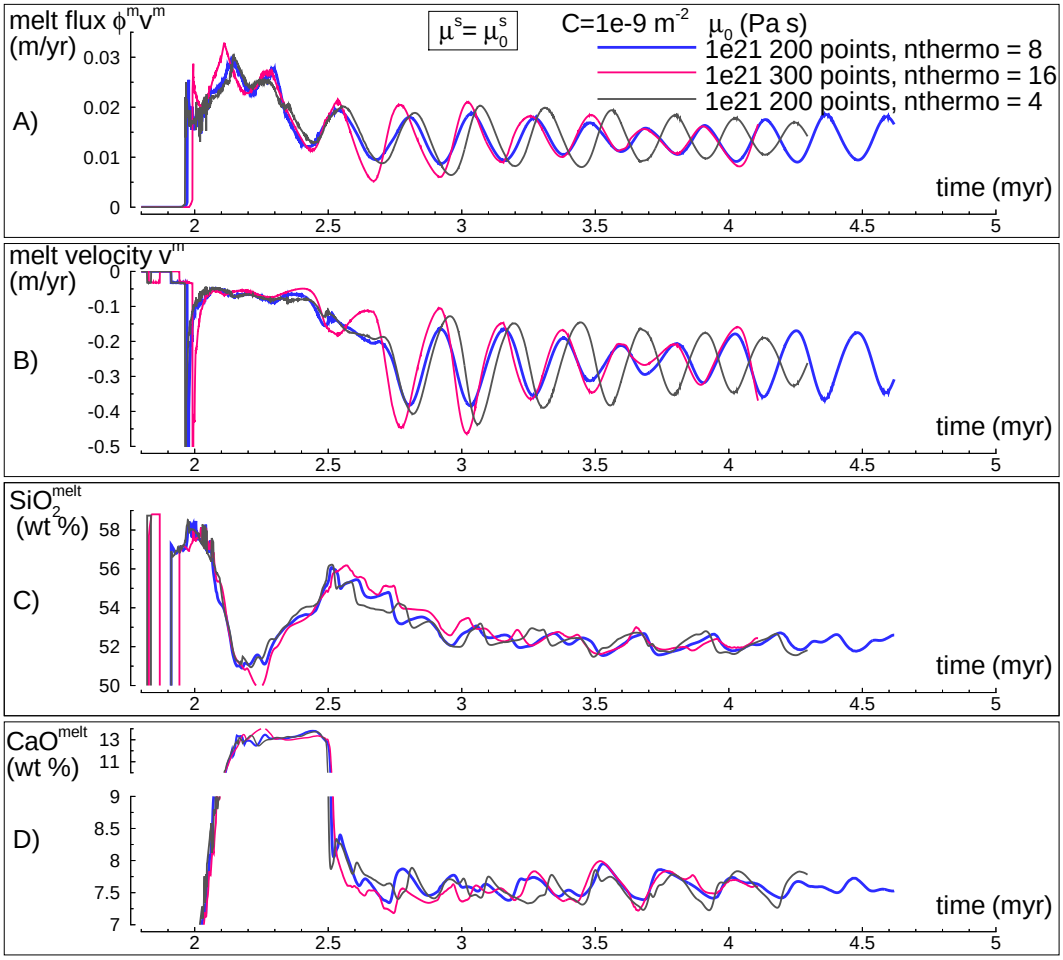

Figure S1. Variation of selected melt properties over time at the top side of the simulation for three models with $\mu^s = \mu_0^s$. The permeability constant is C=10^{-9} m^{-2}, μ_0^s is set to 10^{21} Pa s. The reference model is the same shown in Figure 7 in the main text (blue line) using 200 grid points and nthermo = 8, blue line. The comparison is made with a model using 300 points, nthermo = 16 and another model with 200 grid points, nthermo = 4. Additional details related to these simulations can be found in Table 1 (main text), `PHASE3-P.YRC4`, `PHASE3-P.YRC5`, `PHASE3-P.YRC6`. Panel A) melt flux ($\phi^m v^m$). Panel B) melt velocity (m/yr). Panel C) melt composition: SiO_2 (wt %). Panel D) melt composition: CaO (wt %). Complete data can be found in `PHASE3-P.YRC4.DAT`, `PHASE3-P.YRC5.DAT` and `PHASE3-P.YRC6.DAT` (zip file `max-front1-data.zip`).

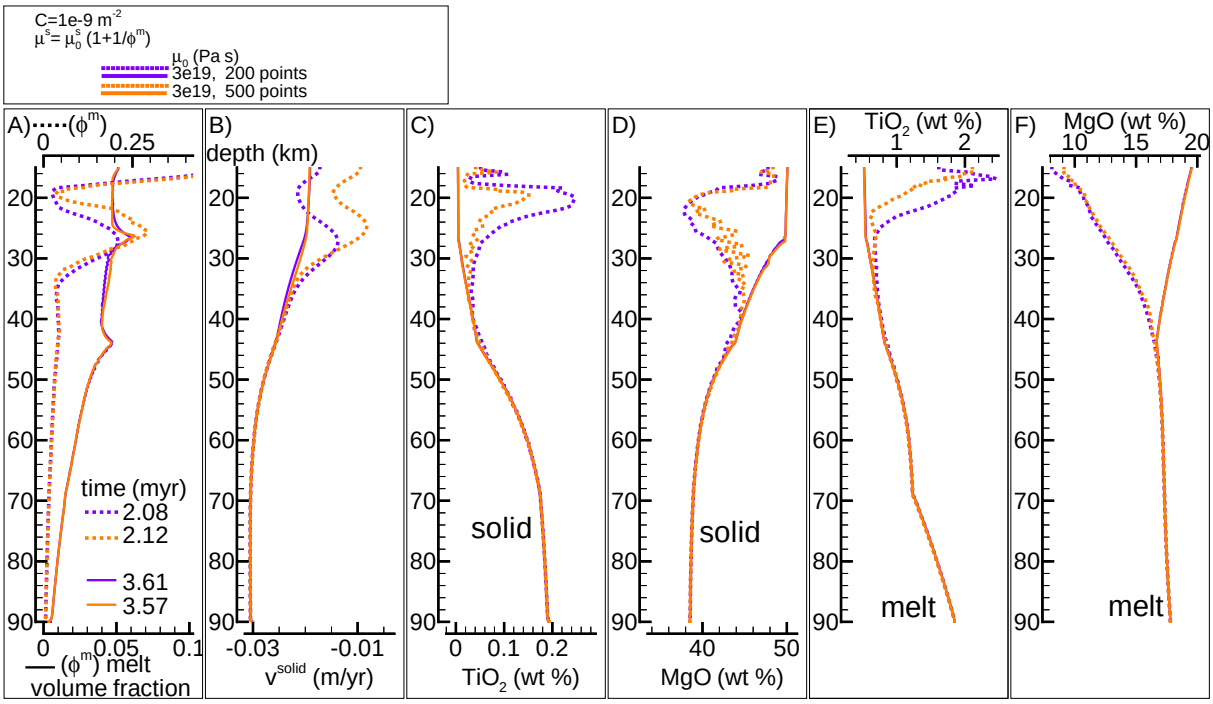

Figure S2. Comparison between two similar simulations with the solid viscosity model: $\mu^s = \mu_0^s(1 + 1/\phi^m)$, $\mu_0^s = 3e19$ Pa s. The first model (purple lines) uses 200 grid points, the thermodynamic computation is applied every 8 time steps. The second model (orange lines) uses 500 grid points, the thermodynamic computation is applied every 16 time steps. Additional details related to these simulations can be found in Table 1 (main text), `PHASE3-P2.YRC14`, `PHASE3-P2.YRC23`. Panel A) melt volume fraction versus depth at 2 different times. Earliest time approximately coincides with the first arrival of melt at the top. Panel B) velocity of the solid matrix. Panel C) variation of TiO_2 in solid (wt %). Panel D) variation of MgO in solid (wt %). Panel E) variation of TiO_2 in melt (wt %). Panel F) variation of MgO in melt (wt %). The complete data for all 12 oxides in melt solid and bulk, at every depth over time are available only for the first simulation, data file `PHASE3-P2.YRC14.DAT` (zip file `max-front1-data2.zip`).

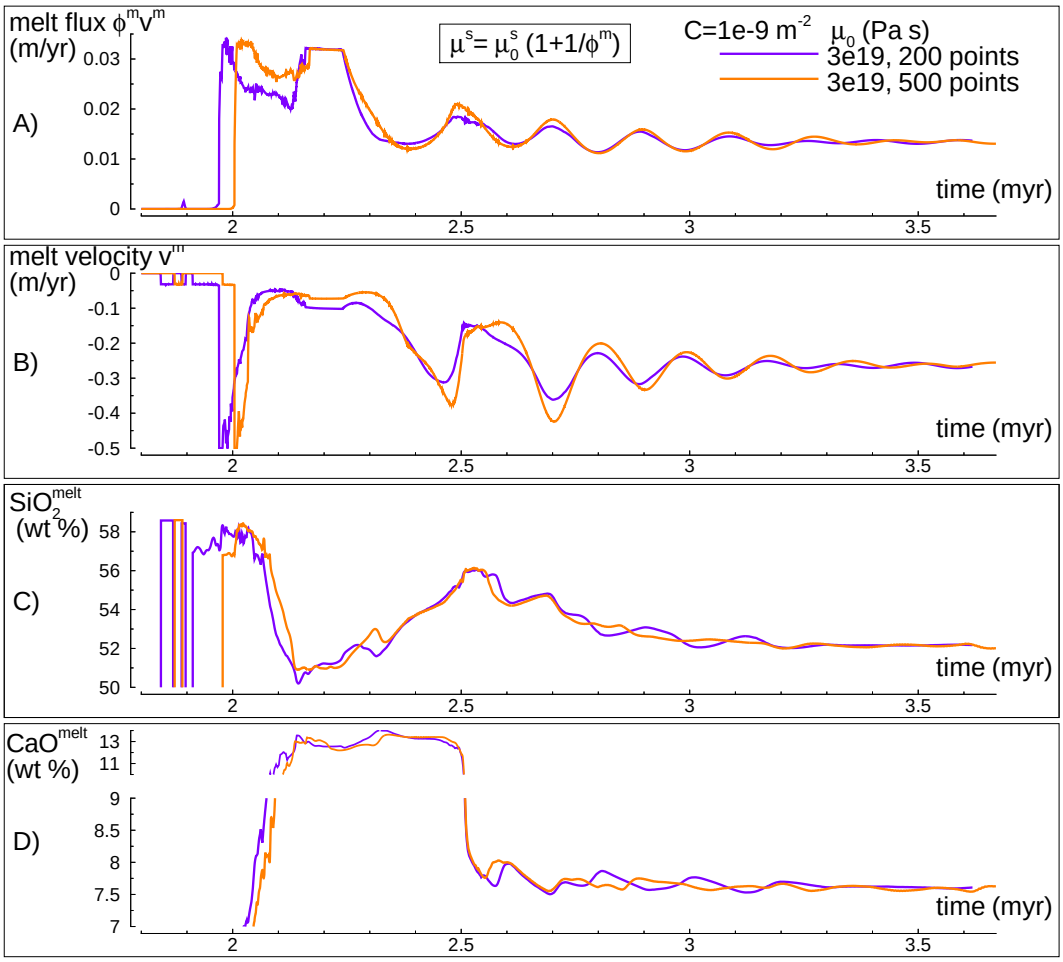

Figure S3. Variation of selected melt properties over time at the top side of the simulation for the two models shown in the previous figure. Details related to these simulations can be found in Table 1 (main text), `PHASE3-P2.YRC14`, `PHASE3-P2.YRC23`. Panel A) melt flux ($\phi^m v^m$). Panel B) melt velocity (m/yr). Panel C) melt composition: SiO_2 (wt %). Panel D) melt composition: CaO (wt %). Complete data for the first model can be found in `PHASE3-P2.YRC14.DAT`, (zip file `max-front1-data2.zip`).

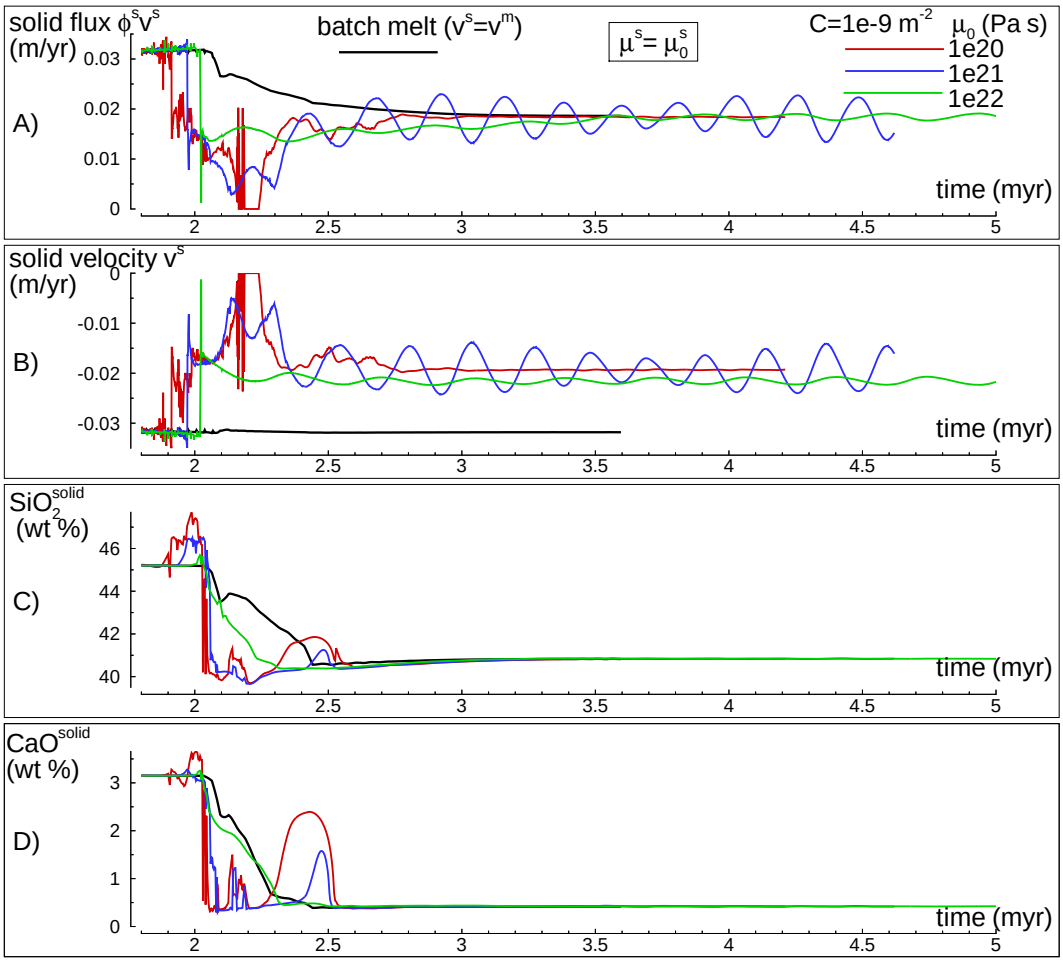

Figure S4. Variation of selected solid mantle properties over time at the top side of the simulation for three models with $\mu^s = \mu_0^s$. The permeability constant is C=10^{-9} m^{-2}, μ_0^s is set to 10^{20}, 10^{21}, 10^{22} Pa s. Results from the batch melting model are also included. The corresponding variations in the melt can be found in Figure 7 (main text). Panel A) solid flux ($\phi^m v^m$). Panel B) solid velocity (m/yr). Panel C) solid composition: SiO_2 (wt %). Panel D) solid composition: CaO (wt %). Complete data `PHASE3-P.BRC4-5.DAT`, `PHASE3-P.YRC7.DAT`, `PHASE3-P.YRC4.DAT` and `PHASE3-P.YRC26.DAT` are included in the zip file `max-front1-data.zip`.